PHYSICAL REVIEW B VOLUME 22, NUMBER 6 15 SEPTEMBER 1980

Configurational model for a one-dimensional ionic conductor

H. U. Beyeler, L. Pietronero, and S. Strässler
Brown Boveri Research Center, CH-5405 Baden, Switzerland
(Received 21 January 1980)

The static and dynamical properties of a Frenkel-Kontorova model (generalized to arbitrary density of defects) are studied. This system with a constant density of particles is intended to describe a one-dimensional ionic conductor. The dynamic properties are studied within a *generalized free-rate theory* in configurational space. (Note that this description does *not* allow for soliton-type transport.) For the case of a piecewise parabolic potential, analytical results are obtained for all the relevant quantities while for a sinusoidal potential numerical results are reported. A refined measurement of the diffuse x-ray scattering for hollandite is presented and interpreted in detail with the above model. This information is then used to compute the effective diffusion barriers and the conductivity that result in good agreement with experiments.

I. INTRODUCTION AND SUMMARY

One of the few features common to most members of the large family of materials exhibiting superionic conduction is the intimate existence of an ordered crystalline lattice and a highly disordered system, i.e., that of the mobile ions. Often the complexity is further enhanced by an incommensurate ratio between the number of available ions and the number of sites available to them. In addition, the density of the mobile particles is generally very high ($>10^{21}$ cm^{-3}) so that their static and dynamic properties are appreciably affected by their mutual interaction. For a theoretical modeling of the static and dynamical properties of such systems it is useful to adopt the Frenkel-Kontorova model[1] generalized to an arbitrary density of effects.[2] This model consists of a chain of harmonically coupled particles embedded in a periodic "substrate" potential. This system may in fact be interpreted as a simplified one-dimensional version of a generalized lattice-gas description of superionic conductors as described in Ref. 3. This lattice-gas concept focuses on the structure of the potential energy in the hyperdimensional configuration space spanned by all coordinates of all particles. Stable equilibrium configurations of the particles in the real space represent minima of the potential energy (containing all interactions between all particles) at the corresponding point in configuration space. It is possible to define a parcellation of the configuration space in volumes, each representing one stable configuration. As a many-body process, the jump of a particle from one site to a neighboring empty one (including the relaxation of the other particles due to the interaction) corresponds then to the transition of the system from the volume of one configuration (in configuration space) to that of another one.

This concept of dynamics corresponds to a generalized rate theory in configurational space.[3] Such a description is valid if the minimum potential barrier (in configurational space) to go from one configuration to another is larger than k_BT and if the damping is large enough so that when the system moves from a given configuration it completely relaxes into a nearest one before a new jump takes place.

In this paper we show that under certain conditions analytical solutions for the static and dynamic properties can be given for such a model; for more complex situations we discuss numerical results. This work has been motivated in part by the desire to demonstrate the practical applicability of the generalized lattice-gas concept[3] and in part by the fact that there are extensive experimental data available on the linear ionic conductor hollandite, a system that represents a close realization of the Frenkel-Kontorova model.

In the second part we thus apply our model to hollandite. Through a fit of the diffuse x-ray scattering spectrum we determine the two relevant microscopic parameters: the ion-host lattice interaction and the ion-ion interaction. Using no further adjustable parameters we then compute the ionic conductivity of hollandite within a generalized rate theory. The result of this calculation is in reasonable agreement with experimental data. We conjecture that the overall very satisfactory agreement between model calculations and experimental data demonstrates the adequacy of the configurational model for the description of this system.

This paper is organized as follows.

(a) In Sec. II we describe the model and the two main assumptions we make: (i) periodic boundary

conditions to preserve local charge neutrality and (ii) generalized rate theory for the dynamical properties. Two types of substrate potentials are considered: a piecewise parabolic one for which analytical results are obtained and a sinusoidal one for which a numerical analysis is performed.

(b) In Sec. III we study the equilibrium properties and show that for the case of a piecewise parabolic potential the problem of determining the static configurations of the Hamiltonian given by Eq. (2.1) can be reduced to an effective spin model with exponential interaction and fixed magnetization. The results are analytical in the sense that, given a configuration only in terms of occupancy of the pots of the potential, the equilibrium displacements of all the particles and the corresponding configurational energy follow [see Eqs. (3.32) and (3.35)]. Of course, in practice, some computer work is still necessary to generate all the possible configurations of a given system. Some of the results of this section have already been briefly reported in a Letter.[2] Here the full derivation is given.

(c) In Sec. IV we extend the description of Sec. III to the saddle-point configurations to determine the effective barrier for diffusion. The transfer rate in configurational space is evaluated for the full many-body system including the effect of thermal fluctuations of all particles. The corresponding conductivity is evaluated neglecting correlation between different configurational changes. It is found that, also for a finite density of defect, a good description of the total conductivity can be obtained in terms of quasiparticles consisting of a vacancy plus the associate distortion field of the surrounding particles.

(d) Section V is dedicated to the analysis of specific results of the model described in the previous sections. A numerical study of the same model with a sinusoidal potential is also reported. These models are applied to study different properties of the one-dimensional ionic conductor hollandite, for which refined data on diffuse x-ray scattering are also presented.

The main features we consider are (i) the stability of configurational states and their contribution to the specific heat, (ii) the reduction of the diffusion barriers due to the interaction between particles, and (iii) the analysis of diffuse scattering and conductivity in hollandite.

II. THE MODEL

We consider a system of mobile interacting ions confined to linear motion and subjected to a periodic substrate potential owing to the crystalline surrounding. If the interaction between the ions is strong enough we can expand the interaction potential around the equilibrium configuration corresponding to no substrate potential and only retain the quadratic terms. The Hamiltonian is then

$$H=\sum_{l=1}^{N}\tfrac{1}{2}m\dot{x}_l^2+\sum_{l=1}^{N}V(x_l)+\tfrac{1}{2}A\sum_{l=1}^{N}(x_{l+1}-x_l-b)^2, \tag{2.1}$$

where x_l denotes the position of the lth ion. The substrate potential V has periodicity a. In general this periodicity is different from b, the periodicity that the interaction between the ions would produce in the absence of the substrate potential.

The first authors to study the dynamical evolution of a Hamiltonian given by Eq. (2.1) with $a=b$ were Frenkel and Kontorova.[1] They pointed out the possibility of soliton-type behavior of such a system. Frank and van der Merwe[4] then studied the equilibrium properties for the discommensurate case ($a\neq b$) with a free-end boundary condition. Recently a number of authors have considered various problems concerning both static and dynamic properties of such a system.[5-14]

Here we study Eq. (2.1) as a representation of a partly filled ionic channel and, in order to preserve charge neutrality (fixed density), we employ *periodic boundary conditions*. This is a very important fact because it gives rise to equilibrium properties different from those corresponding to free-end boundary conditions as studied in Ref. 5. For the dynamical properties we study Eq. (2.1) within a *generalized rate theory*.[3,15,16] This has the following physical meaning: We assume that the interactions between the mobile ions and the ions of the fixed substrate give rise, in addition to the potential V, to a damping acting on our mobile ions. Eventually a stochastic force should be added to this description in order to preserve thermal equilibrium.[17] This damping is assumed to be small enough so that the vibrational properties of our system are not overdamped. At the same time it is assumed to be large enough so that when the system moves from one configuration to another (adjacent), it completely relaxes in the new configuration before a new jump takes place. This means, for example, that if an ion or, in general, a collective coordinate moves from one potential well to another, it thermalizes in this new well without preserving any memory of the transfer.[18-24] As one can see, this approximation *does not allow* for the so-called "soliton motion" often associated with equations of type (2.1).[13] By its nature, soliton motion involves successive correlated jumps of the system

through several wells, an effect which is not believed to be of importance in linear ionic conductors,[11] but there exist different opinions on this point.[7]

If these conditions for the damping are satisfied, the transport properties can be given from a generalized rate theory and they are *independent* on the damping itself. For this reason we omit any dissipative term in Eq. (2.1). It is important to note that, even in the case of no external damping mediated by the potential V, a fluctuation from equilibrium also decays into the vibrational modes of Eq. (2.1).[25-27] This means that an intrinsic damping always exists for fluctuations that bring the system from one configuration to another even if no damping exists for phonons. This again supports the use of a rate theory.

With respect to the unit cell of length a defined by the period of the substrate potential, the density of ions is

$$\rho = a/b = N/N_s \tag{2.2}$$

with N_s being the number of pots defined by the periodic potential (one pot per unit cell).

In order to obtain exact analytical results, it is convenient to define the periodic potential as a piecewise parabolic potential

$$V(x) = \begin{cases} V(x+a), \\ \frac{1}{2}m\omega_0^2 x^2, \quad |x| < \frac{1}{2}a. \end{cases} \tag{2.3}$$

Numerical results will also be presented for a sinusoidal potential. The dependence of the results on the specific form of the potential will be discussed but we shall see that in general it is rather small.

Assuming that a pot can be occupied by one ion only, we introduce the variable

$$p_l = 0, 1, 2, \ldots, \tag{2.4}$$

which denotes the number of empty pots which follow the lth ion. A particular configuration of the system is defined by the set

$$\alpha = \{p_l\}. \tag{2.5}$$

The relation between average particle density ρ and p is easily obtained by noting that in the p representation the number of pots is given by

$$N_s = \sum_{l=1}^{N} (1 + p_l) = N(1 + \langle p \rangle). \tag{2.6}$$

This gives

$$\langle p \rangle = (1/\rho) - 1. \tag{2.7}$$

It is convenient to introduce the relative coordinate δx_l that represents the displacement of the lth atom from the bottom of its pots. From the definition of p_l we can write

$$x_l = \sum_{l'=1}^{l} (p_{l'} + 1)a + \tfrac{1}{2}a + \delta x_l \tag{2.8}$$

and therefore

$$x_{l+1} - x_l = a(p_l + 1) + \delta x_{l+1} - \delta x_l. \tag{2.9}$$

We have then

$$\begin{aligned}(x_{l+1} - x_l - b)^2 = {} & (\delta x_{l+1} - \delta x_l)^2 \\ & + 2(\delta x_{l+1} - \delta x_l)[a(p_l + 1) - b] \\ & + [a(p_l + 1) - b]^2. \end{aligned} \tag{2.10}$$

The third term is a constant and we will neglect it. Using Eq. (2.7) and writing (from now on) x_l instead of δx_l we can rewrite the total potential as

$$\begin{aligned} V = {} & \sum_{l=1}^{N} \tfrac{1}{2}m\omega_0^2 x_l^2 + \tfrac{1}{2}A \sum_{l=1}^{N} (x_{l+1} - x_l)^2 \\ & + aA \sum_{l=1}^{N} (x_{l+1} - x_l)(p - \langle p \rangle). \end{aligned} \tag{2.11}$$

We study now the static configurations corresponding to the potential given by Eq. (2.11). A complication arises from the fact that a given configuration $\alpha = \{p_l\}$ may not satisfy the condition $\delta V^\alpha = 0$ within the limits $|x_l| < a/2$. For the moment we introduce an extended substrate potential adjusted to every configuration. This potential has the form of Eq. (2.3) for each pot but it extends beyond the limits $|x_l| < a/2$. The configurations that make use of this extension of the potential are unstable with respect to the original potential given by Eq. (2.3) and we will eliminate them later.

III. EQUILIBRIUM PROPERTIES OF CONFIGURATIONS

In this section we study the static equilibrium properties (zero temperature). The results we derive here are analytical and allow us, given a configuration α, to specify all the ionic displacements at equilibrium and the corresponding total potential energy.

For a given configuration α, the equilibrium positions are given by the condition

$$\delta V^\alpha = 0, \tag{3.1}$$

where the potential is the one given by Eq. (2.11) with the extension of the background potential as discussed at the end of Sec. II.

It is convenient to write the displacement x_l as a Fourier series with respect to the index l:

$$x_l = \frac{1}{\sqrt{N}} \sum_q e^{iql} Q_q, \tag{3.2}$$

where Q_q is the qth Fourier component of x_l,

$$Q_q = \frac{1}{\sqrt{N}} \sum_l e^{-iql} x_l . \tag{3.3}$$

Because of the periodic boundary conditions, q only takes the values

$$q = \frac{2\pi}{N} n \quad (n = 0, 1, 2, \ldots, N) . \tag{3.4}$$

By using Eq. (3.2) we have

$$x_{l+1} - x_l = \frac{1}{\sqrt{N}} \sum_q e^{iql} (e^{iq} - 1) Q_q \tag{3.5}$$

and

$$\sum_l (x_{l+1} - x_l)^2 = 2 \sum_q (1 - \cos q) Q_q Q_{-q} . \tag{3.6}$$

Similarly we have

$$\sum_l x_l^2 = \sum_q Q_q Q_{-q} . \tag{3.7}$$

The potential given by Eq. (2.11) can now be rewritten as

$$V = V_0 + V_1 \tag{3.8}$$

with

$$V_0 = \sum_q \tfrac{1}{2} m \phi(q) Q_q Q_{-q} , \tag{3.9}$$

$$\phi(q) = \omega_0^2 [1 + g(1 - \cos q)] , \tag{3.10}$$

$$g = 2A / m \omega_0^2 , \tag{3.11}$$

and

$$V_1 = aA \sum_q (e^{iq} - 1) Q_q \zeta_{-q} , \tag{3.12}$$

having defined

$$\zeta_q = \frac{1}{\sqrt{N}} \sum_l e^{-iql} (p_l - \langle p \rangle) . \tag{3.13}$$

The equilibrium conditions [Eq. (3.1)] give

$$\frac{\partial V}{\partial Q_{q'}} = \frac{\partial V_0}{\partial Q_{q'}} + \frac{\partial V_1}{\partial Q_{q'}} = 0 , \tag{3.14}$$

where

$$\frac{\partial V_0}{\partial Q_{q'}} = \sum_q \tfrac{1}{2} m \phi(q) \left(Q_{-q} \frac{\partial Q_q}{\partial Q_{q'}} + Q_q \frac{\partial Q_{-q}}{\partial Q_{q'}} \right)$$

$$= m \phi(q') Q_{-q'} \quad [\phi(q) = \phi(-q)] \tag{3.15}$$

and

$$\frac{\partial V_1}{\partial Q_{q'}} = Aa (e^{iq'} - 1) \zeta_{-q'} . \tag{3.16}$$

From Eq. (3.14) we obtain the equilibrium value Q_q^0 for each Fourier coefficient once the configuration is given. There results

$$Q_q^0 = -\frac{Aa}{m \phi(q)} (e^{-iq} - 1) \zeta_q . \tag{3.17}$$

The corresponding potential energy is given by substituting Eq. (3.17) into the total potential given by Eqs. (3.8)–(3.13). This gives

$$V_0 = \frac{1}{N} \sum_q \tfrac{1}{2} m \phi(q) \left(\frac{Aa}{m \phi(q)} \right)^2 (e^{-iq} - 1)(e^{iq} - 1) \zeta_q \zeta_{-q} , \tag{3.18}$$

$$V_1 = \frac{1}{N} aA \sum_q (e^{iq} - 1) \left(\frac{-Aa}{m \phi(q)} \right) (e^{-iq} - 1) \zeta_q \zeta_{-q} , \tag{3.19}$$

and

$$V = V_0 + V_1 = -\frac{(Aa)^2}{2m} \sum_q \frac{1}{\phi(q)} (2 - e^{iq} - e^{-iq}) \zeta_q \zeta_{-q} . \tag{3.20}$$

By inserting Eq. (3.13) into Eq. (3.20) we obtain

$$V = \frac{Aa^2}{2} \sum_{l,l'} [B(l - l' + 1) + B(l - l' - 1) - 2B(l - l')] \times (p_l - \langle p \rangle)(p_{l'} - \langle p \rangle) , \tag{3.21}$$

where

$$B(n) = \frac{1}{N} \frac{A}{m} \sum_q e^{iqn} \frac{1}{\phi(q)} . \tag{3.22}$$

For large N we can write

$$B(n) \simeq \frac{1}{2\pi} \int_0^\pi \frac{\cos(ny) dy}{(1 + 1/g) - \cos y} = \frac{\alpha^{|n|+1}}{1 - \alpha^2} , \tag{3.23}$$

where

$$\alpha = 1 + (1/g)(1 - \sqrt{1 + 2g}) . \tag{3.24}$$

Of the various terms of Eq. (3.21), only the term containing $p_l p_{l'}$ is different from zero since

$$\sum_{l'} [B(l - l' + 1) + B(l - l' - 1) - 2B(l - l')] = 0 . \tag{3.25}$$

It is convenient to introduce

$$C(n) = 4g [B(n + 1) + B(n - 1) - 2B(n)] . \tag{3.26}$$

We now have two possibilities:

(a) $n = 0$,

$$C(0) = [8\alpha/(1 - \alpha)^2] 2(\alpha - 1) B(0)$$
$$= [16\alpha/(\alpha - 1)] B(0) , \tag{3.27}$$

(b) $n \neq 0$,

$$C(n) = [8\alpha/(1 - \alpha)^2](\alpha + 1/\alpha - 2) B(n)$$
$$= 8B(n) . \tag{3.28}$$

The term (a) only gives a constant term that we omit. The potential energy of a given configuration can then be rewritten as

$$V=\frac{1}{8g}\,Aa\sum_{l,l';l\neq l'}C(l-l')p_l p_{l'}\,, \tag{3.29}$$

and defining

$$C'(n)=\alpha^{|n|}=e^{-|n|/\lambda} \tag{3.30}$$

with

$$\lambda=[\ln(1/\alpha)]^{-1}\,, \tag{3.31}$$

we finally have

$$V=\tfrac{1}{2}J\sum_{l,l';l\neq l'}C'(l-l')p_l p_{l'}\,, \tag{3.32}$$

where

$$J=8J_0\frac{\alpha}{(1-\alpha^2)} \tag{3.33}$$

and

$$J_0=\tfrac{1}{2}m\omega_0^2(\tfrac{1}{2}a)^2 \tag{3.34}$$

is the barrier height of the periodic potential.

It is clear from Eq. (3.32) that the problem is now reduced to a one-dimensional spin model with exponential interaction, where the magnetization is fixed by the value of the particle density ρ. We remember that the only approximation made until now is the avoidance of double occupancy of a site.

Given a configuration we can also compute the equilibrium displacements of all the atoms by inserting Eq. (3.17) into Eq. (3.2). This gives

$$\begin{aligned}x_l^{(0)}&=\frac{1}{N}\sum_q e^{iql}\left(\frac{-Aa}{m\phi(q)}\right)(e^{-iq}-1)\sum_{l'}e^{-iql'}(p_{l'}-\langle p\rangle)\\&=-a\sum_{l'}[B(l-l'-1)-B(l-l')](p_{l'}-\langle p\rangle)\,.\end{aligned} \tag{3.35}$$

At this point we have to remember that this result is based on the virtual extended substrate potential, and to remove this additional assumption, Eq. (3.35) has to be completed with the condition

$$|x_l|\leq\tfrac{1}{2}a\,,\quad l=1,\ldots,N\,. \tag{3.36}$$

If this condition is not fulfilled, the corresponding configuration represents no equilibrium state of the system.

Equations (3.32), (3.35), and (3.36) constitute the final results of this section. Given a configuration $\alpha\equiv\{p_l\}$, these equations provide directly the static equilibrium displacements of all particles and the total potential energy. They form the basis for the systematic calculation of all static equilibrium states of a system from which such properties as thermal occupancies, x-ray structure factors, or the specific heat follow in a straightforward fashion.

IV. CONDUCTIVITY

In this section we derive analytical results for the conductivity of our system using a generalized rate theory. The conditions for the validity of this approach have been discussed in Sec. II.

The conductivity corresponding to a generalized rate theory contains two terms.[3] One is independent of the frequency and it is this one we explicitly consider here. The other term is frequency dependent and vanishes for high frequencies. It accounts for correlation between different hops in configurational space. This second term is omitted here but we point out that in general it can give a finite contribution at zero frequency.[3,18-24] The frequency-independent term gives in our case[3,24]

$$\sigma^{(0)}=\frac{1}{2k_BT}\frac{1}{\Omega}\sum_{\alpha,\alpha'}p_\alpha^0\,\overline{\Gamma}_{\alpha\alpha'}(l_{\alpha\alpha'})^2\,, \tag{4.1}$$

where Ω is the volume of our system, α indicates a configuration as defined by Eq. (2.5), and $l_{\alpha\alpha'}$ is the difference in dipole moment between the configurations α and α'. The term $\overline{\Gamma}_{\alpha\alpha'}$ represents the average transition rate from the configuration α to α'. Its definition in the general case of three dimensions and N particles is[3]

$$\begin{aligned}&\overline{\Gamma}_{\alpha\alpha'}=\langle\Gamma_{\alpha\alpha'}\rangle_\alpha\,,\\&\Gamma_{\alpha\alpha'}=\int_{S_{\alpha\alpha'}}\delta^{3N}(\vec{q}-\vec{q}_s)(\vec{v}\cdot\vec{n}_{\alpha\alpha'})\Theta(\vec{v}\cdot\vec{n}_{\alpha\alpha'})\,dS\,,\end{aligned} \tag{4.2}$$

where $\langle\cdots\rangle_\alpha$ is the thermal average within configuration α. The terms $\vec{q}=\{x_l\}$ and $\vec{v}=\{\dot{x}_l\}$ represent the position and velocity of the system. The integration in Eq. (4.2) is over the common surface $S_{\alpha\alpha'}$ of the volumes (in configurational space) corresponding to the configurations α and α', $\vec{n}_{\alpha\alpha'}$ is the normal to this surface in the direction $\alpha\to\alpha'$, and Θ is the Heaviside step function.

In order to illustrate how Eq. (4.2) works, we first apply it to the case of independent particles in one dimension and reproduce the standard result of absolute rate theory.[16] For independent particles we have

$$\sigma^{(0)}=\frac{e^2n_c}{k_BT}\,\overline{\Gamma}\,a^2\,, \tag{4.3}$$

where n_c is the concentration of particles. From Eq. (4.2) we have in this case

$$\overline{\Gamma}=\langle v\Theta(v)\rangle\langle\delta(x-\tfrac{1}{2}a)\rangle\,. \tag{4.4}$$

We have

$$\langle v\Theta(v)\rangle = \frac{\int_0^\infty v\exp\left(-\frac{mv^2}{2k_BT}\right)dv}{\int_0^{+\infty}\exp\left(-\frac{mv^2}{2k_BT}\right)dv} = \left(\frac{k_BT}{2\pi m}\right)^{1/2}, \tag{4.5}$$

$$\langle\delta(x-\tfrac{1}{2}a)\rangle = e^{-J_0/k_BT}\Big/\int_{-a/2}^{a/2}\exp\left(-\frac{m\omega_0^2x^2}{2k_BT}\right)dx \simeq e^{-J_0/T}\Big/\left(\frac{2k_BT}{m\omega_0^2}\right)^{1/2}, \tag{4.6}$$

where $J_0=\frac{1}{2}m(\frac{1}{2}a)^2$. The approximation in Eq. (4.6), valid if $k_BT/J_0<1$, consists in extending the limits of integration from $-\infty$ to $+\infty$. We obtain

$$\bar{\Gamma} = \frac{\omega_0}{2\pi}e^{-J_0/k_BT} \tag{4.7}$$

that is the standard result.

We consider now the evaluation of the rate as given by Eq. (4.2) for the case of the system described in Sec. II. It is convenient to split the Hamiltonian into

$$H = H_c + H_p, \tag{4.8}$$

where the configurational part H_c is given by Eq. (2.32) and the phonon part is

$$H_p = \sum_{l=1}^{N}\left[\tfrac{1}{2}m\dot{u}_l^2 + \tfrac{1}{2}A(u_{l+1}-u_l)^2 + \tfrac{1}{2}m\omega_0^2u_l^2\right], \tag{4.9}$$

having defined

$$u_l = x_l - x_l^{(0)},$$

where $x_l^{(0)}$ represents the equilibrium displacement as given by Eq. (2.35).

Given a configuration $\alpha\equiv\{p_l\}$, its configurational energy is given [using Eq. (2.32)] by $E_\alpha = H_c(\{p_l\})$. We consider now the elementary process that leads from a configuration α to a configuration α'. We assume, for example, that this corresponds to the motion of the particle l into a nearest free pot. Of course this is not just a one-particle process because the equilibrium positions of all the other particles are affected through the coupling with the particle l. The activation energy is defined by the potential energy of the system in the unstable saddle-point configuration for which the particle l is somewhere halfway between its original pot and the adjacent one. The difference between this energy and E_α defines the activation energy $U_{\alpha\alpha'}$. In order to explicitly evaluate this energy it is convenient to define a force f_l that acts on the particle l. The displacement of a general particle l' where the particle l is subjected to the force f_l can be computed from Eq. (4.9) by using a Fourier expansion in analogy to the derivation of Eq. (2.35). The result is

$$u_{l'} = f_l\frac{1}{N}\sum_q\frac{e^{iq(l-l')}}{\phi(q)} = \frac{f_l}{m\omega_0^2}\frac{2B(l-l')}{g}. \tag{4.10}$$

The activation energy is then written as

$$U_{\alpha\alpha'} = \int_0^{a/2-x_l^{(0)}} f_l\,du_l = J_0\left(\frac{2x_l^{(0)}}{a}+1\right)^2\frac{g}{2B(0)}. \tag{4.11}$$

The conditions for $U_{\alpha\alpha'}$ to exist are

$$p_l\neq 0, \qquad |x_l^{(0)}|\leq\tfrac{1}{2}a, \quad |x_l^{(0)}+u_{l'}|\leq\tfrac{1}{2}a. \tag{4.12}$$

The rate for a transition $\alpha\to\alpha'$ can be computed from

$$\bar{\Gamma}_{\alpha\alpha'} = \left(\frac{k_BT}{2\pi m}\right)^{1/2}\langle\delta(u_l+x_l^{(0)}-\tfrac{1}{2}a)\rangle_\alpha. \tag{4.13}$$

It is convenient to rewrite the potential energy as

$$V = \sum_{l,l'}V_{l,l'}u_lu_{l'}, \qquad V_{ll'} = \tfrac{1}{2}[\phi(l,l')+\phi'(l,l')], \tag{4.14}$$

where

$$\phi(l,l') = \delta_{l,l'}m(\omega_0^2+\omega_1^2), \qquad \phi'(l,l') = -\tfrac{1}{2}m\omega_1^2(\delta_{l+1,l'}+\delta_{l-1,l'}), \tag{4.15}$$

and we have introduced

$$\omega_1^2 = A/m. \tag{4.16}$$

For convenience we now let the coordinate $l=0$ be the "jumping" coordinate. For a fixed u_0 we obtain from Eq. (4.14) a new potential energy

$$\tilde{V} = \sum_{l,l'\,(l,l'\neq 0)}V_{l,l'}\tilde{u}_l\tilde{u}_{l'}, \tag{4.17}$$

where now $\tilde{u}_l$ indicates the relative displacement with respect to u_l given by Eq. (4.10) when u_0 is fixed by the delta function appearing in Eq. (4.13). We now have from Eq. (27)

$$\bar{\Gamma}_{\alpha\alpha'} = \left(\frac{k_BT}{2\pi m}\right)^{1/2}e^{-U_{\alpha\alpha'}/k_BT}\Phi, \tag{4.18}$$

where

$$\Phi = \frac{\int\prod_{l\neq 0}d\tilde{u}_le^{-\tilde{U}/k_BT}}{\int\prod_l d\tilde{u}_le^{-U/k_BT}}. \tag{4.19}$$

The explicit evaluation of Eq. (4.19) can be carried out analytically using for the integrations the ex-

tended harmonic potentials in analogy with Eq. (4.5). The calculation, rather long, is not reported here.[28] The result is

$$\Phi = \omega_\alpha \left(\frac{m}{2\pi k_B T}\right)^{1/2}, \tag{4.20}$$

$$\omega_\alpha = \frac{1}{2}\,\frac{\omega_0^2+\omega_1^2+[(\omega_0^2+\omega_1^2)^2-\omega_1^4]^{1/2}}{[(\omega_0^2+\omega_1^2)^2-\omega_1^4]^{1/4}}. \tag{4.21}$$

Note that for $\omega_1 = 0$ we obtain

$$\omega_\alpha = \omega_0, \quad U_{\alpha\alpha'} = J_0 \tag{4.22}$$

in agreement with Eq. (4.7).

For the case of a single vacancy Eq. (4.11) becomes

$$U_{\alpha\alpha'} = J_0 s. \tag{4.23}$$

A single vacancy behaves thus as an effective particle seeing an effective barrier reduced by s compared to the single-particle barrier J_0, where

$$s = \frac{1-\alpha}{1+\alpha}. \tag{4.24}$$

For a low concentration of vacancy the conductivity thus becomes

$$\sigma = \sigma_0 e^{-J_0 s/k_B T} f(s), \tag{4.25}$$

where

$$\sigma_0 = \frac{e^2 a^2 n_h}{k_B T}\left(\frac{\omega_0}{2\pi}\right), \quad n_h = n_0(1-\rho), \tag{4.26}$$

where n_h is the density of holes and n_0 is the density of potential minima. $f(s)$ contains all the nontrivial prefactor corrections due to many-particle effects; from Eq. (4.21) follows

$$f(s) = [\tfrac{1}{2}(1+s)]^2 (1/s^{3/2}). \tag{4.27}$$

Note that in Eq. (4.26) we have used the fact that $|l_a - l_b| = a$.

For an arbitrary density of holes the conductivity is given by

$$\sigma = \sigma_0 e^{-J_0 s/k_B T} f(s) \rho F, \tag{4.28}$$

where $\rho = a/b$. We have then

$$f(s)\rho F = \frac{\sum_{\alpha\alpha'} e^{-(E_\alpha + U_{\alpha\alpha'})/k_B T}}{\sum_{\alpha\alpha'} e^{-E_\alpha/k_B T}}. \tag{4.29}$$

The numerical evaluation of Eq. (4.29) gives a rather smooth behavior $F \simeq 1$ for $k_B T/J_0 > 0.1$ and $\rho > 0.75$ with deviations of less then 10%. The implication of this result is that the description of conductivity in terms of an appropriate "effective" single-particle picture as given by Eq. (4.25) can be extended to the full many-body problem [as given by Eq. (4.29)] in a rather wide parameter region.

V. APPLICATIONS AND DISCUSSION

In this section we will illustrate some specific results for the model described by Eq. (2.1). In order to obtain analytical expressions for various properties it was necessary to use a substrate potential that is piecewise parabolic [Eq. (2.3)]. To evaluate the significance of the results obtained with such a highly simplified potential we have, in addition, performed fully numerical calculations with a sinusoidal potential of the form

$$V_s(x) = C_s \sin^2[(\pi/a)x]. \tag{5.1}$$

These calculations made use of an adapted least-squares routine to determine all minima of the 13-dimensional configuration space.

We, in particular, determined the parameters that best describe the experimental data available on the hollandite. In the composition $K_{2x}Mg_x Ti_{8-x}O_{16}$ hollandite consists of an octahedral (Ti, Mg) oxide framework forming separate linear channels in which the potassium ions reside. Each channel contains one site per unit cell along the tetragonal c axis ($c = 2.97$ Å) and the fractional occupancy ρ of these sites is equal to x. The single-crystal samples used for the diffuse-scattering experiments were grown by a flux method and had a composition corresponding to $\rho = 77\%$.[29] In our model we restrict the calculations to the case of 13 particles within 17 wells, resulting in a fractional occupancy of $\rho = 0.765$, very close to the experimental value. We have verified that differently sized models with about the same ρ give very similar results.

A. Stability of configurational states

Without ion-ion interaction, our model system of 13 particles in 17 wells possesses $\binom{17}{13} = 2380$ energetically degenerate configurational states with the particles located at the local well minima. Introducing an ion-ion interaction leads to an energy splitting between these states and causes the equilibrium positions of the particles to be shifted off the well minima. For a strong interaction, certain configurations will no more fullfill Eq. (3.36); i.e., certain particles are shifted to a position outside their assigned well. This means that there is no more local minimum of the potential energy within that part of the configuration space corresponding to the starting configuration. This "configuration quenching" turns out to be of considerable importance in the case of hollandite. In order to discuss the results it is convenient to introduce

$$C_I = \tfrac{1}{2} A a^2 \tag{5.2}$$

as a measure of the interaction energy and C_s

[Eq. (5.1)] and $C_p = \frac{1}{8} m\omega_0^2 a^2$ as the energy barriers for the sinusoidal and parabolic potential, respectively.

In Figs. 1 and 2 we show how the total number of stable configurations depends on the strength of the interaction relative to the strength of the periodic potential for the sinusoidal and the parabolic potential. The number of states is normalized to that of the interactionless system (i.e., 2380). To display the energy spreading of the states, Figs. 1 and 2 also give the number of states existing in the 13-particle system with a total energy up to 1, 2, or 3 barrier heights. The results describe the complete transition from a nearly interactionless highly disordered system to a strongly interacting and highly ordered system. The plateau in the total number of states between $1.3 \leq C_I/C_s \leq 3$ for the sine-wave potential and between $3 \leq C_I/C_p \leq 5$ for the parabolic potential is due to the fact that in these ranges there remain all configurations with vacancies as next-nearest neighbors or further apart.

Once the various stable configurations with the associate energies are known, one can compute the configurational contribution to the specific heat. This problem has been specifically discussed in Ref. 2 where it is shown that small groups of configurational states are a realization of the two- (or few-) level systems introduced phenomenologically by Phillips and Anderson *et al.*[30] to explain the linear specific heat observed at low temperatures (0.1–1 K) in disordered systems.[31] In this respect we remark that, in our model, the gap between two configurational states can become extremely small, keeping the parameters within a reasonable range.[2] In connecting these configurational excitations to the low-temperature extra-specific heat, one should also note that at very low temperature ($T \lesssim 1$ K) thermodynamic equilibrium cannot be reached for all the configurations and the statistical problem has to be factorized into the groups of configurations for which equilibrium is achieved. This is necessary to obtain a linear specific heat. In Ref. 2 we have simply used Boltzmann statistics and, in fact, it was not possible to obtain a linear contribution to the specific heat over an extended region of temperatures. For the case of hollandite, these configurational excitations are, in addition, expected to produce a peak in specific heat at intermediate temperatures[2] (40–100 K).

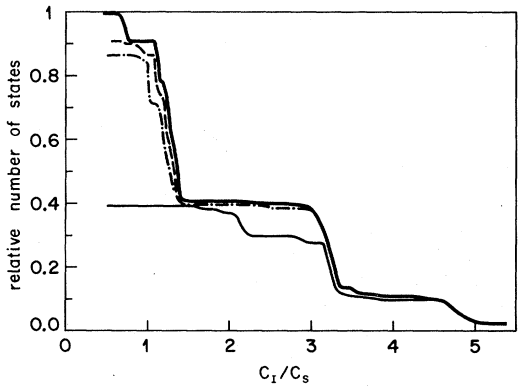

FIG. 1. The upper line shows the relative number of stable configurations as a function of the ratio between interaction energy and potential barrier for the case of a sinusoidal potential. The other lines give the number of states with a total energy to 1, 2, or 3 barrier heights (C_s).

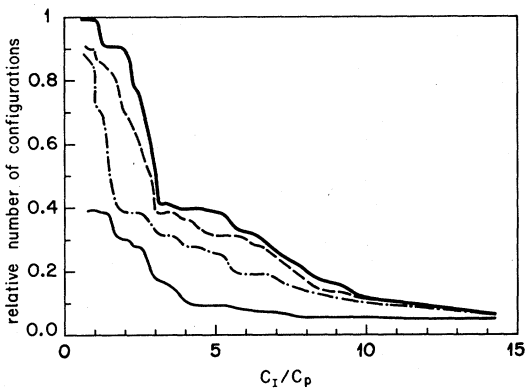

FIG. 2. Same as Fig. 1 for a piecewise quadratic potential.

B. Displacive order and effective diffusion barriers

To given values of C_I and C_s (C_p) and a given temperature corresponds a completely defined state of order of our model system. It is interesting in this respect to look in Figs. 3 and 4 at the relation between the ratios C_I/C_s (C_I/C_p) and the displacement of ions adjacent to a vacancy in the ground state of our 17-well model system. The ground state is given by the most regular distribution of vacancies, e.g., on the sites 1, 5, 9, and 13, the displacement is then taken as the average displacement of the ions in wells 2, 4, 6, 8, 10, 12, 14, and 17.

As discussed in Sec. IV the barrier for diffusion is given by the difference of the energy of the *total* system between an initial equilibrium configuration and a saddle-point configuration. In configuration space this saddle point is located on the border between the volumes assigned to the initial (α) and the final (α') equilibrium configurations. In our model there is a great number of such saddle points, each connecting two adjacent

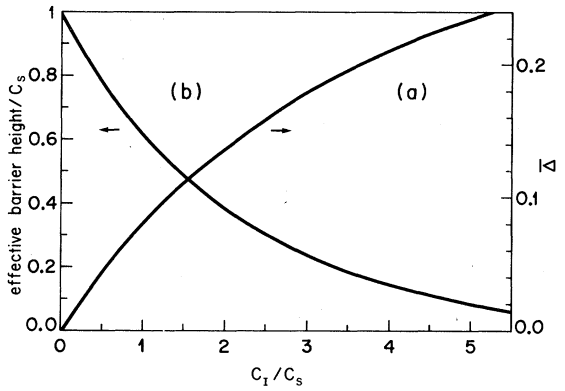

FIG. 3. For the sinusoidal potential we show here (a) (right) the average fractional displacement ($\overline{\Delta}$) of the ions adjacent to a vacancy in the ground state and (b) (left) the effective barrier height for diffusion ($U_{\alpha\alpha'}/C_s$) as functions of the ratio between interaction energy and potential barrier.

configurations. For zero interaction, all particles see identical diffusion barriers C_s and C_p for sinusoidal and parabolic potential, respectively. We show here, in a specific example, how the effective barriers with interaction can drastically differ from the "naked" barriers given by the framework potential. For this purpose we focus on a single transition leading from one ground-state configuration to an equivalent one (see Fig. 5). In Figs. 3 and 4 is shown the factor by which the effective barrier is reduced below the framework barrier in functions of the ratios C_I/C_s and C_I/C_p, the ratio between interaction and framework potential. We note that in the range where the interaction just tolerates the existence of next-nearest-neighbor vacancies the barriers are typically reduced by a factor of 2.

It should be noted at this point that the effect of the reduction of diffusion barriers due to the interaction between particles has been studied

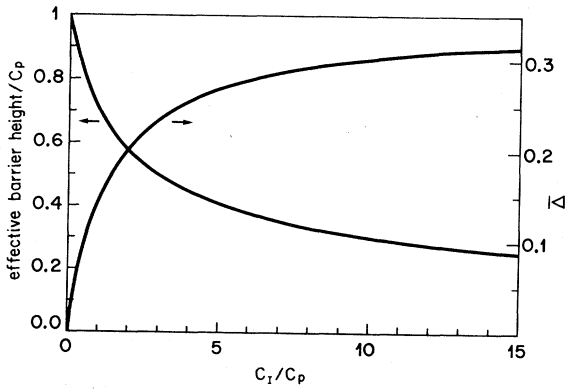

FIG. 4. Same as Fig. 3 for a piecewise quadratic potential.

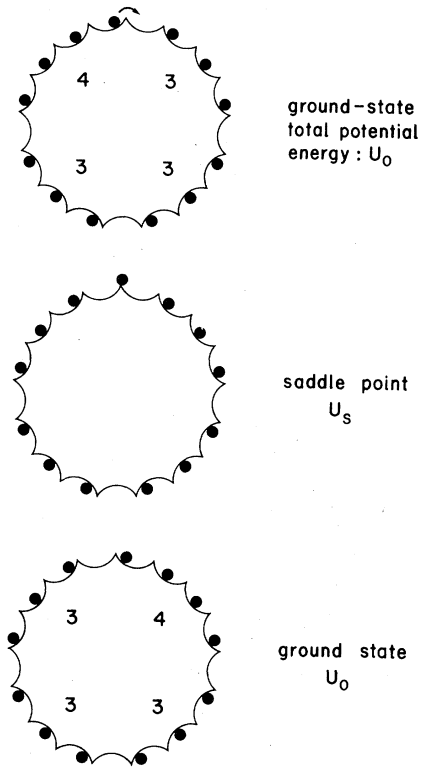

FIG. 5. Schematic illustration of the transition between two degenerate configurations.

by various authors[6,7,11] and it seems to play an important role also in β-alumina.[32]

C. Diffuse scattering in hollandite

From our calculations the x-ray scattering of a configuration α is given by

$$I^{\alpha}(s) = \sum_{l,l'} f_K f_K^* \exp[-2\pi i s(x_l^{(\alpha)} - x_{l'}^{(\alpha)})], \quad (5.3)$$

where f is the scattering factor of a potassium ion (we neglect Debye-Waller factors which do not add any new local structure). The total static x-ray scattering of the mobile subsystem due to configurational disorder is then

$$I^{\mathrm{tot}}(s) = \sum_{\alpha} p_{\alpha} I^{\alpha}(s), \quad (5.4)$$

where p_α is probability for the system to be in configuration α.

As shown in Refs. 29 and 33, hollandite exhibits at room temperature a planar diffuse-scattering pattern which could conclusively be linked to the partial cationic order within the channels. We base our analysis on the experimental interference function $F(s) = C_F I_{\mathrm{expt}}(s)/(f_K f_K^*)$, where C_F is a correction factor accounting for polarization effects at the monochromator and at the sam-

ple, and f_K is the complex scattering factor of a potassium ion. The diffuse-scattering intensity has been determined on c^*, the reciprocal channel axis using Mo $K\alpha$ radiation and an LiF monochromator. For the quantitative analysis an accurate knowledge of the true linewidths of the diffuse structure will be crucial. For the present work the scattering has thus been reexamined with higher resolution in order to obtain a spectrum whose features are not resolution limited. Figure 6 shows the new spectrum on which we base the present analysis.

For the following discussion it is helpful to recall the two main conclusions from the earlier interpretations of the diffuse scattering[33]:

(i) The relative intensity of the diffuse peaks at 0.77 and 1.77 reciprocal-lattice units (rlu) indicates that ions adjacent to a vacancy are displaced towards the latter by about 0.24 lattice constants.

(ii) The distribution of the vacancies is far from random; they favor mutual separations of four or five lattice units.

We have determined the best fit to the diffuse scattering by computing Eq. (5.4) for both the sinusoidal and the parabolic potential. As to be expected, the relative intensity of the diffuse structures is directly related to the ratios C_I/C_p as those ratios determine the displacements of the ions. The best fit of the peak heights is achieved with $C_I/C_s = 5$ and $C_I/C_p = 3.2$, respectively. From Figs. 3 and 4 we deduce relative displacement of 0.23 and 0.24 for the vacancy-neighboring ions in agreement with the value determined in Ref. 33. Figure 1 shows that for the sine-wave potential and the determined value of C_I/C_s there are only very few stable configurations left; for the parabolic potential there exist all configurations with vacancies at least two lattice units apart (Fig. 2).

The absolute values of the potentials determine the population of these configurations and therefore the amount of occupational disorder. Experimentally, information about the occupational disorder and thus about the strength of the potentials (relative to kT_{expt}) is contained in the linewidths of the diffuse structures. Although every care has been taken to obtain a spectrum not affected by experimental resolution, the error margin in the linewidths is certainly larger than that in the line intensities. Further, the model system with 17 potential wells is just barely large enough to describe the observed disorder; it yields a resolution in reciprocal space of $\frac{1}{17}$ rlu and this is only slightly less than the widths of the diffuse structures.

With all these precautions in mind, one deduces $C_s \sim 0.15$ eV and $C_p \sim 0.23$ eV from the fit. From Figs. 2 and 4 we may finally extract a reduction factor for the effective barrier of 0.1 and 0.4 for the sinusoidal and the parabolic potential, respectively.

We have, to this point, purposely given in parallel the data for both potential shapes in order to display the range of uncertainty of the model-

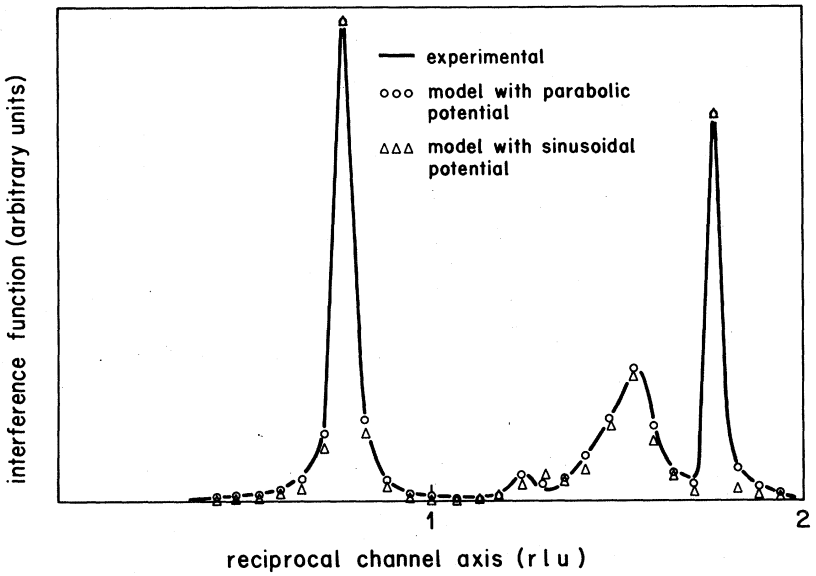

FIG. 6. New refined diffuse x-ray scattering for hollandite. The continuous line refers to the experimental data while the points refer to the theoretical models with long-range interaction as given by Eq. (5.5). (rlu = reciprocal-lattice units).

derived microscopic parameters. Microscopically, the framework potential is mainly determined by the interaction between the potassium ions and the surrounding oxygens. Steric considerations show that for ions on top of the barriers the hard-core repulsive interaction between potassium and oxygen is dominant. We must thus expect the walls of the potential wells to be steeper than given by a sine function but certainly not as pointed as a parabolic potential.

D. A more realistic interaction potential for hollandite

Our model [Eq. (2.1)] only includes short-range interactions and it is not obvious that the true Coulomb-type interaction between mobile ions can be reproduced by effective short-range interactions. We have thus repeated the numerical-model analysis of the hollandite data using a long-range ion-ion interaction of the type

$$V_{II'} = \frac{e^2}{|x_I - x_{I'}| \epsilon_{\text{eff}}(|x_I - x_{I'}|)} , \tag{5.5}$$

where we derive $\epsilon_{\text{eff}}(r)$ from the picture of a dielectric double cylinder[33]: We assume that within a radius r_0 around the channel axis the effective dielectric constant ϵ_i is given by the electronic polarizability of the potassium ions (the ionic displacive contribution is not to be included, as the model explicitly contains the displacive short-range order). Outside r_0 the dielectric constant ϵ_a is assumed to be that of the bulk framework structure. From this model follows the effective dielectric constant for the interaction between two charges on the cylinder axis straightforwardly. For small separations it is equal to ϵ_i, for large separations it approaches ϵ_a. The transition occurs at $r \sim r_0$. For hollandite we assume $\epsilon_i \sim 2$, $\epsilon_a \sim 100$ (deduced from the far-ir reflectivity). The large framework polarizability is due to a strong coupling of the oscillation of the Ti atoms within the oxygen octahedra to electronic states. r_0 should be of the order of the distance between the channel axis and the closest Ti atoms, i.e., $r \sim 3$–4 Å. For these numbers the interaction between nearest- and next-nearest neighbor is just in the transition range of $\epsilon_{\text{eff}}(r)$ (1 lattice unit in hollandite is equal to 2.97 Å). Thus the interaction sensitively depends on the value of r_0.

As a test of the sensitivity of model-derived microscopic parameters on the particular form of the ion-ion interaction, and in order to obtain a most realistic set of parameters for hollandite, we have repeated the fitting procedure using Eq. (5.5) as interaction and considering r_0 as an adjustable parameter. The best-fitting diffuse spectra are shown in Fig. 6. The model parameters are given in Table I. Comparing the parameters to those corresponding to short-range interactions it becomes evident that the inclusion of the long-range interaction requires a substantial lowering of the framework potential in order to arrive at the degree of disorder reflected in the diffuse x-ray scattering. For the sinusoidal potential this effect leads to a situation where there exist only 12 stable configurations; these do not enable a fit of the observed linewidths. One has thus to conclude that within our model the experimental data are not consistent with a sinusoidal potential. On the other hand, the fitted parabolic potential certainly represents an upper bound to the true potential.

E. Conductivity

The very satisfactory agreement between model-derived and experimental diffuse scattering supports the adequacy of the configurational model for the description of the state of order in hollandite. Independent of the specific type of framework and interaction potential, the determined

TABLE I. In this table we summarize the "best-fit" parameters for the various models considered in this paper. The most realistic is probably the case of parabolic background potential with long-range interactions between the mobile ions.

	Harmonic (short-range) interaction		Long-range interaction [Eq. (5.5)]	
	sinusoidal	parabolic	sinusoidal	parabolic
Framework potential strength (C_s and C_p)	0.15 eV	0.23 eV		0.144 eV
Barrier-reduction factor	0.1	0.4	0.08	0.45
Effective barrier height	0.015 eV	0.092 eV		0.065 eV
$\bar{\Delta}$	0.23	0.24	0.231	0.242
Interaction strength C_I	0.75 eV	0.74 eV	see text	
r_0				2.3 Å

parameters clearly show the eminent importance of the ion-ion interaction. Through configuration quenching and configurational energy splitting of the stable states it leads to a relatively high degree of order, but it also reduces the barriers for diffusion by more than a factor 2 as compared to the naked framework potential barriers. These phenomena are of course greatly affecting the dynamic properties of the system. While the configuration quenching severely limits the number of possible ionic jumps, the barrier reduction greatly enhances the jump rates for those processes that connect two stable configurations. Taking the parabolic barrier of 0.065 eV as an upper limit we conjecture that the real potential barrier is in the range between 0.04 and 0.05 eV, i.e., not too much above k_BT at room temperature. Comparing this value to the activation energies of conductivity usually found in superionic conductors (0.15–0.25 eV), it appears surprisingly low, even lower than the barrier height in the archetype superionic conductor α-AgI (~0.07 eV).

This surprising result calls for an independent experimental verification. As shown in Ref. 34, up to rather high frequencies the conductivity of hollandite is dominated by the existence of extrinsic barriers hindering the long-range ionic motion in the channels. From a certain high frequency on, the motion will be confined to the unperturbed segments between the extrinsic barriers and one should then be able to observe the intrinsic conductivity corresponding to that discussed in Sec. IV. Estimates indicate that this transition from the anomalous, defect-barrier-dominated-conduction regime to the regular intrinsic diffusive regime should occur in the range of 10^9–10^{10} Hz. Preliminary conductivity results at 9×10^9 Hz in fact already indicate an intrinsic activation energy of the order of 0.037 eV and a conductivity (at $T=300$ K) $\sigma \gtrsim 0.5$ $(\Omega\,\mathrm{cm})^{-1}$.[35] Using the experimental value for the effective barrier with a reduction factor $s\sim0.5$ we get a naked barrier $J_0=0.037/s=0.074$ eV. From Sec. IV we have [Eq. (4.28)]

$$\sigma=\sigma_0 e^{-J_0 s/k_BT} f(s)\rho F \tag{5.6}$$

with

$$\sigma_0=e^2a^2n_h/k_BT\,. \tag{5.7}$$

As discussed at the end of Sec. IV for $\rho\gtrsim 75$ and $k_BT/J_0>0.1$, we have $F\sim1$. The other parameters are

$$a=2.97\ \text{Å}\,,\quad \rho=0.77 \tag{5.8}$$

and

$$n_h=n_0(1-\rho)=1.52\times10^{21}\ \mathrm{cm}^{-3}\,, \tag{5.9}$$

where n_0 is the density of potential pots. From Eq. (4.27) we have then

$$f(s=0.5)=1.58\,. \tag{5.10}$$

With these values we obtain

$$\sigma_0(T=300\ \mathrm{K})\simeq 6.8\ (\Omega\,\mathrm{cm})^{-1} \tag{5.11}$$

and

$$\sigma(T=300\ \mathrm{K})\simeq 2.1\ (\Omega\,\mathrm{cm})^{-1}\,. \tag{5.12}$$

Being aware of both the difficulty to obtain accurate experimental conductivities at 10^{10} Hz and that to derive this quantity from a microscopic theory we only use parameters derived from structural data, the agreement can be termed fair.

[1] J. Frenkel and T. Kontorova, J. Phys. (Moscow) 1, 337 (1939).

[2] L. Pietronero and S. Strässler, Phys. Rev. Lett. 42, 188 (1979).

[3] H. U. Beyeler, P. Brüesch, L. Pietronero, W. R. Schneider, S. Strässler, and H. R. Zeller, in *Physics of Superionic Conductors*, edited by M. Salamon (Springer, Berlin, 1979), Vol. 15, p. 77.

[4] F. C. Frank and J. H. van der Merwe, Proc. R. Soc. London Ser. A 198, 205 (1949).

[5] J. A. Snyman and J. H. van der Merwe, Surf. Sci. 42, 190 (1974).

[6] J. C. Wang and D. F. Pickett Jr., J. Chem. Phys. 65, 5378 (1976).

[7] J. B. Sokoloff, Phys. Rev. B 16, 3367 (1977); 17, 4843 (1978); J. B. Sokoloff, and A. Widom, *ibid.* 18, 2824 (1978); T. Geisel, in *Fast Ion Transport in Solids*, edited by P. Vashishta *et al.* (North-Holland, New York, 1979).

[8] M. B. Fogel, S. E. Trullinger, A. R. Bishop, and J. A. Krumhansl, Phys. Rev. Lett. 24, 1411 (1976).

[9] E. Stoll, T. Schneider, and A. R. Bishop, Phys. Rev. Lett. 42, 937 (1979), and references therein.

[10] R. A. Guyer and M. D. Miller, Phys. Rev. Lett. 42, 718 (1979).

[11] L. Pietronero and S. Strässler, Solid State Commun. 27, 1041 (1978).

[12] M. Remoissenet, Solid State Commun. 27, 681 (1978).

[13] *Solitons in Condensed Matter*, edited by A. R. Bishop and T. Schneider (Springer, Berlin, 1978).

[14] D. Baeriswyl and A. R. Bishop (unpublished).

[15] C. P. Flynn, *Point Defects and Diffusion* (Clarendon, Oxford, 1972).

[16] H. A. Kramers, Physica (Utrecht) 7, 284 (1940); C. A. Wert, Phys. Rev. 79, 601 (1950); G. H. Vineyard, J. Phys. Chem. Solids 3, 121 (1957); P. B. Visscher, Phys. Rev. B 13, 3272 (1976); 14, 347 (1976).

[17] For the case of a single particle, see P. Fulde, L. Pie-

tronero, W. R. Schneider, and S. Strässler, Phys. Rev. Lett. 35, 1776 (1975); W. Dieterich, I. Peschel, and W. R. Schneider, Z. Phys. B 27, 177 (1977).
[18]In the limit of infinitely fast transfer (here we do *not* use this simplification) the dynamics of the system become simply a hopping. Examples of this description can be found in Refs. 3, and 19–24.
[19]W. Dieterich, I. Peschel, and W. R. Schneider, Commun. Phys. 2, 175 (1977).
[20]P. M. Richards, Phys. Rev. B 16, 1393 (1977).
[21]H. Sato, in *Solid Electrolytes*, edited by S. Geller (Springer, Berlin, 1977), and references therein.
[22]D. L. Huber, Phys. Rev. B 15, 533 (1977).
[23]J. C. Kimball and L. W. Adams Jr., Phys. Rev. B 18, 5851 (1978).
[24]L. Pietronero, S. Strässler, and H. R. Zeller, Solid State Commun. 30, 305 (1979); *ibid.* in *Fast Ion Transport in Solids*, edited by P. Vashishta *et al.* (North-Holland, New York, 1979), p. 165; L. Pietronero and S. Strässler, Z. Phys. B 36, 263 (1980).
[25]M. B. Fogel, S. E. Trullinger, A. R. Bishop, and J. A. Krumhansl, Phys. Rev. B 15, 1587 (1977).
[26]W. Atkinson and N. Cabrera, Phys. Rev. A 3, 763 (1965).
[27]N. Theodorakopoulos, Z. Phys. B 33, 385 (1979); J. C. Kimball (unpublished).
[28]W. R. Schneider and S. Strässler (unpublished).
[29]H. U. Beyeler, Phys. Rev. Lett. 37, 1557 (1976); H. U. Beyeler and C. Schüler, Solid-State Ionics (in press).
[30]W. A. Phillips, J. Low Temp. Phys. 7, 351 (1972); P. W. Anderson, B. I. Halperin, and C. M. Varma, Philos. Mag. 25, 1 (1972).
[31]R. O. Pohl and G. L. Solinger, Ann. N.Y. Acad. Sci. 279, 150 (1976); R. B. Stephens, Phys. Rev. B 13, 852 (1976).
[32]J. C. Wang, M. Gaffari, and S. Choi, J. Chem. Phys. 63, 772 (1975).
[33]H. U. Beyeler, L. Pietronero, S. Strässler, and H. J. Wiesmann, Phys. Rev. Lett. 38, 1532 (1977).
[34]J. Bernasconi, H. U. Beyeler, S. Strässler, and S. Alexander, Phys. Rev. Lett. 42, 819 (1979).
[35]S. H. Khanna, G. Grüner, R. Orbach, and H. U. Beyeler (unpublished).